International Journal of Multidisciplinary Research and Development
Online ISSN: 2349-4182, Print ISSN: 2349-5979, Impact Factor: RJIF 5.72
www.allsubjectjournal.com
Volume 3; Issue 5; May 2016; Page No. 111-119

Forest carbon stock assessment at Barkot Flux tower Site (BFS) using field inventory, Landsat-8 OLI data and geostatistical techniques

*** T Watham, SPS Kushwaha, S Nandy, NR Patel, S Ghosh**

Indian Institute of Remote Sensing, ISRO 4- Kalidas Road, Dehradun, Uttarakhand, India

Abstract

Quantification of forest biomass is of vital importance to assess productivity - a critical information for carbon budget accounting, carbon flux monitoring and for understanding the forest ecosystem response to climate change. In this present study, we used field measured aboveground biomass (AGB), Landsat 8 OLI (operational land imager) derived variables and geostatistical tools for spatial total biomass and carbon stock mapping surrounding Barkot Flux Site (BFS), Uttarkhand, India. For this purpose, different AGB prediction maps were produced using on Ordinary Kriging (OK), Universal Kriging (UK), Co-Kriging (CoK) and Regression Kriging (ReK) methods and tested the models' accuracy. Biomass estimated using OK and UK had root mean square error (RMSE) of 121.78 and 139.48 Mg ha^{-1}, respectively. Total 16 variables were tested one by one as an auxiliary variable in the CoK technique. CoK with Land Surface Water Index (LSWI) had the lowest RMSE of 58.77 Mg ha^{-1} (R^2=0.63). LSWI performed best because of its sensitivity to leaf moisture. Also, ReK method was tested using top three variables (based on RMSE value) achieved in CoK method. However, ReK was not able to improve the accuracy, attained by CoK. This may be due to high spectral variability or the limitation of the typical OK method. Under performance by OK and the UK must have been due to their prerequisite of a large number of well-distributed sample points to capture adequately the spatial variability. Therefore, selection of site-specific suitable variables and method can help in improving the accuracy of biomass assessment. Hence, CoK method with LSWI as an auxiliary was considered for biomass and carbon stock estimation. The total carbon stock (47 % of the total biomass) in the study area was estimated to be 2240797.37 Mg C, with an average of 276.13 Mg C ha^{-1}. Furthermore, the estimated spatial biomass/carbon will be useful in complementing Eddy Covariance (BFS) and remote sensing based carbon dynamics studies being carried out in the same study area.

Keywords: Carbon, Biomass, Barkot Flux Site (BFS), Kriging, Land surface water index (LSWI).

1. Introduction

Forests are relevant to climate change issues due to their capability to act as reservoirs of carbon. Carbon is stored in the forest as biomass in organic matter (living and dead) both below and above ground including trees, the understorey, dead wood, litter, and in soil. Forest biomass mapping is useful in quantifying the carbon emissions due to forest degradation [1], forest planning and management [2], and in policy making [3]. Realizing the significance of forests in climate change mitigation strategies, the UNFCCC [4]. stressed the need of efficient monitoring system using a combination of remote sensing and the ground-based forest inventory for the greenhouse gases (GHGs) emission and sequestration due to forest cover change. Information about forest stand and the quantification of biomass are of great importance to assess the forest ecosystem productivity, work out carbon budget, and better understand the role forests in the global carbon cycle perspective.

Satellite remotely sensed data are generally available at the pixel level of any area under investigation, in contrast to the field measurements of forest variables known only for the sampled part of the area [5]. This pixel information has been widely used in retrieving forest biophysical parameters, monitoring vegetation biomass and productivity at different scales [6-8]. The statistical relationship between forest parameters and remotely sensed data products are used to generate an aboveground biomass (AGB) map [11]. The most common method for estimation of AGB is the regression analysis between vegetation indices based on red and near-infrared (NIR) wavelengths with field measured AGB [10-12]. In tropical and subtropical regions, where biomass and species diversity are high, use of vegetation indices has met with moderate success [13, 14]. Recent years, non-parametric techniques *viz.,* ANN, *k*-NN, etc. became very popular for assessing the AGB [15, 16]. A drawback of many of these methods that use remotely sensed data for forest inventory is that these techniques do not consider the inherent auto-correlated nature of forest [17]. or the distribution pattern of the underlying forest parameters. With the use of parametric and semi-parametric techniques such as Ordinary Kriging (OK), Universal kriging (UK), Co-Kriging (CoK) and Regression Kriging (ReK), spatially correlated nature of forest can be taken into consideration for improving the forest biomass/carbon. However, their use in forestry is still relatively limited [18]. Meng *et al.* [19] used Landsat ETM+ images for auxiliary data and found the performance of multi-variable kriging better than univariate kriging for prediction of the pine stand basal area. ReK resulted in a low error and the high coefficient of determinant (R^2). Ver Hoef *et al.* [20] compared the spatial linear predictors including OK and UK and *k*-NN: using artificial populations and resampled forestry data, and demonstrated the superiority of spatial linear predictions over *k*-NN. Tsui *et al.* [21] integrated airborne Lidar and space-borne radar data and found UK better than CoK in predicting the AGB. Existing literature indicates no definite consensus on the advantages of various kriging methods or other prediction techniques with the use of satellite data.

In present study, we estimated and mapped forest carbon stock surrounding Barkot Flux Site (BFS) using field inventory, Landsat-8 OLI (operational land imager) data, and various geostatistical techniques. And we tried to explore, specifically,

1. the use of simple spatial auto-correlation that exists in nature using OK and UK,
2. the potential of different remotely sensed variables (individual spectral bands as well as vegetation and water indices) towards the prediction of biomass, and
3. combination of spatial auto-correlation and the covariance that exist between variable of interest (biomass) and the other variables in CoK and ReK method for carbon stock estimation.

2. Materials and Methods

2.1 Study area and climate

This study was conducted at surrounding Barkot Flux site (BFS), which comprises two forest ranges of Dehradun district, here after referred as Barkot forest. The study area consists of two adjacent forest ranges of Barkot and Rishikesh, covering an area of 84.96 km^2 (30°03′52′′-30°10′43′′N and 78°09′49′′-78°17′09′′E) (Figure 1). Champion and Seth [22] described Barkot forest under Sub-Group-3C, North Indian Tropical Moist Deciduous Forest, and forest type being Moist Bhabar Dun Sal Forest - 3C/C2b. We also found sal (*Shorea robusta*) as the dominant species in this area. The underwood is generally light and consists of rohini (*Mallotus philippensis*), chamror (Ehretia laevis), and amaltas (*Cassia fistula*). Monsoon usually begins by the third week of June and continues until September with an average annual rainfall of ~2300 mm. The climate is typically tropical and humid. The on-site observed temperature ranged between 2°C (in January) to 41°C (in June) during 2014.

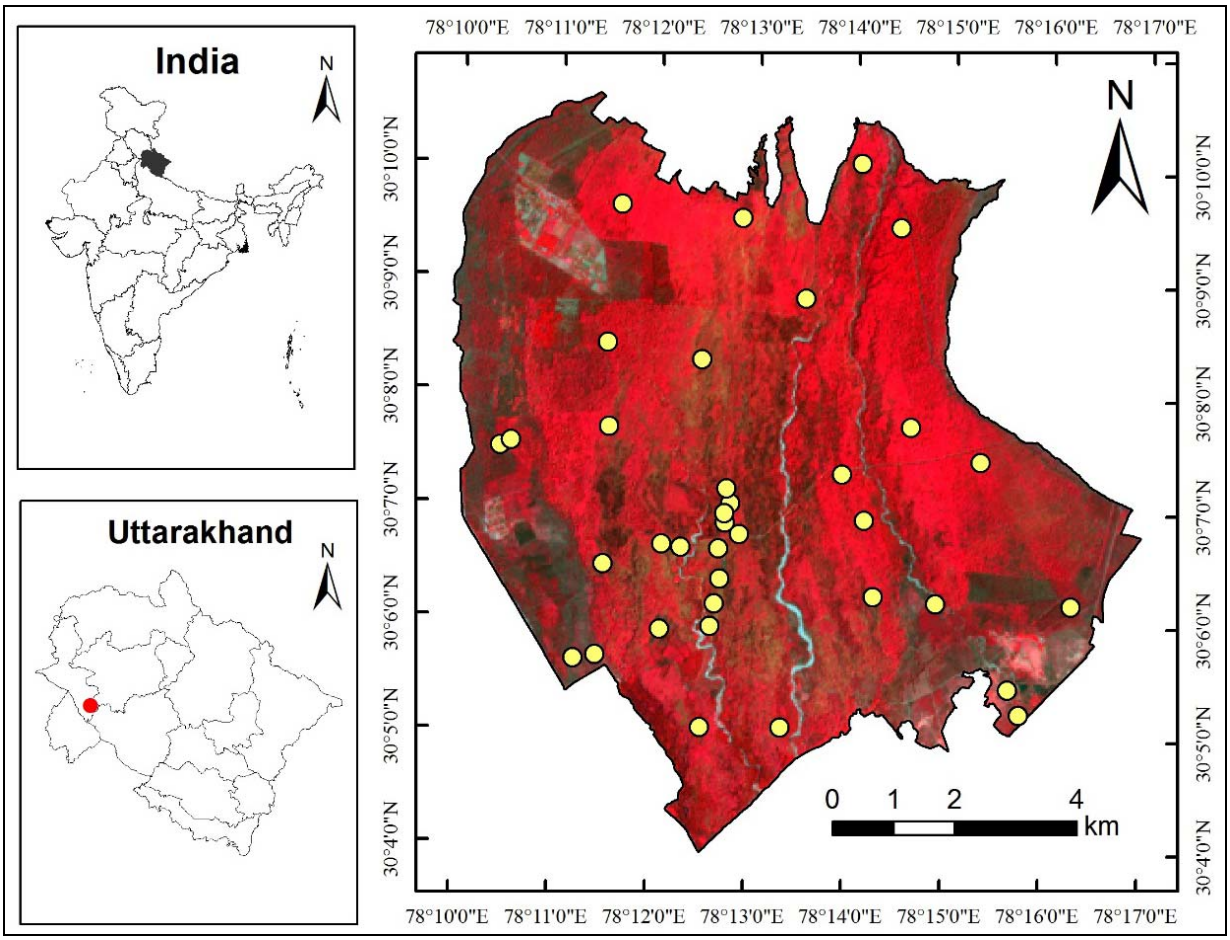

Fig 1: Location of the study area with overlaid field sample points.

2.2 Methods

Landsat-8 OLI satellite data of April 11, 2013 was used during this study. Digital numbers were converted to reflectance values as per standard method described in Landsat-8 data users handbook version 1 (http://landsat.usgs.gov/documents/Landsat8DataUsersHandbook.pdf). Henceforward, only the obtained reflectance data was further used for all the processing. Altogether 16 satellite derived variables *viz.*, green band (0.533-0.590 µm), red band (0.636-0.673 µm), near infra-red (0.851-0.879 µm), shortwave infrared (SWIR)-1 (1.566-1.651 µm) and SWIR-2 (2.107-2.294 µm), one principle component (PC) layers obtained from above mentioned bands and ten Vegetation Indices (VIs) listed in Table 1 were used in this study.

On-screen visual image interpretation of the standard false colour composite on 1:50,000 scale was carried out for stratification of different vegetation types/land cover and canopy density categories. Three canopy density classes, *viz.*, very dense (> 70 %), moderately dense (40-70%) and open (10-40%), were delineated. Stratified random sampling method was adopted to lay out sample plots in different type-density strata for field inventory. A pilot survey was conducted to

calculate the required number of sample plots using following formula [23]:

$$N = \frac{t^2 \times (CV)^2}{(SE\%)^2}$$

Where, N is the number of sample plots, t is the statistical value at 95 % significance level, CV is the coefficient of variation, and SE% is the standard error percentage.

Table 1: List of different satellite data derived indices.

Indices	Formula	Remarks
Midir	$\frac{SWIR1}{SWIR2}$	Musick & Pelletier, 1988 [24]
Msi	$\frac{SWIR1}{NIR}$	Hunt Jr. & Rock, 1989 [25]
Lswi-1	$\frac{NIR-SWIR1}{NIR+SWIR1}$	Xiao *et al.*, 2002 [26]
Lswi-2	$\frac{NIR-SWIR2}{NIR+SWIR2}$	Xiao *et al.*, 2002 [26]
Ndvi	$\frac{NIR-RED}{NIR+RED}$	Rouse *et al.*, 1974 [27]
Wdrvi	$\frac{\propto *NIR-RED}{\propto *NIR+RED}+\frac{1-\propto}{1+\propto}$	Peng and Gitelson 2011 [28] ($\propto$ was set as 0.2)
Evi	$2.5*\frac{NIR-RED}{NIR+6*RED+7.5*BLUE+1}$	Huete *et al.*, 2002 [29]
Vari	$\frac{GREEN-RED}{GREEN+RED-BLUE}$	Gitelson *et al.*, 2002 [30]
Rdvi	$\frac{NIR-RED}{SQRT(NIR+RED)}$	Rougean & Breon, 1995 [31]
Osavi	$\frac{NIR-RED}{NIR+RED+0.16}$	Rondeaux *et al.*, 1996 [32]

MidIR= Mid-infrared, MSI =Moisture Stress Index, LSWI = Land Surface Water Index, NDVI = Normalised Differential Vegetation Index, WDRVI = Wide Range Vegetation Index, EVI = Enhanced Vegetation Index, RDVI = Renormalized Difference Vegetation Index, OSAVI = Optimised Soil Adjusted Vegetation Index.

Minimum of 33 sample plots was required. A total of 36 sample plots were laid in different strata. Out of which, approx. 70 % (26) of the plots were randomly selected for testing and the remaining approx. 30 % plots (10) were used for validation purpose. The total number of sample plots were proportionately distributed in each of the stratum using following formula:

$$n_h = \frac{N_h}{N} \times n$$

Where, n_h= number of samples in h stratum, N_h= size of h stratum, N = total population size and n = total number of samples.

Field inventory was carried out in square plots size of 0.1 ha (31.62 m×31.62 m). At each sample plot, species name, Girth at Breast Height (*gbh*) of all trees at 1.37 m above ground and canopy density were noted down. Two sample plots of 5 m x 5 m for shrubs at opposite corners, 5 sample plots of 1 m x 1 m for herbs and litters at four corners and one 1 m x 1 m at the center of the plot for were also laid in each sample plot. A total number of individuals for each shrub species were noted, and specimen samples (including roots) for each species were collected. Litter at each 1 m x 1 m plot was weighted onsite using electronic balance and noted, and only 100 g of litter was collected as a representative sample. Representative samples of each shrub species and litters were kept in hot air oven at 80°C for drying till constant weight and finally total shrub biomass for every species and litter was calculated for each plot. Herbs in each 1m x 1m plot was harvested and oven-dried. Schematic of field inventory is given in Fig. 2.

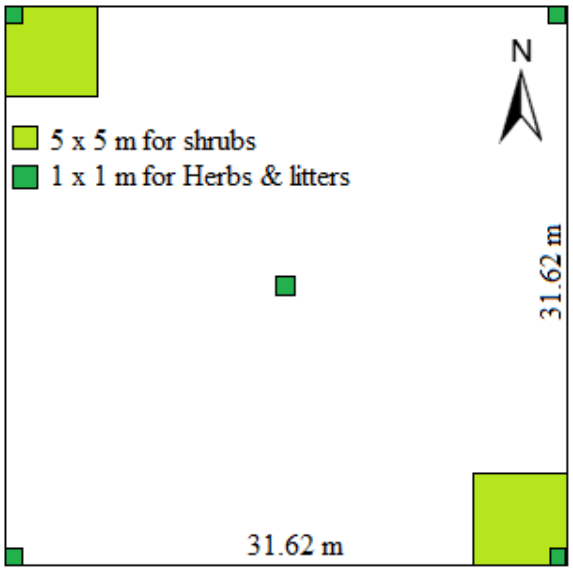

Fig 2: Schematic of field inventory for carbon stock estimation.

The volume of each individual tree in sample plot was calculated by using Diameter at Breast Height (*dbh*) (from *gbh*) value in the specie-specific volumetric equations developed by the Forest Survey of India [33]. The AGB was

obtained by multiplying the trees volume with specific gravity [34] of the wood of the tree species and further multiplying by biomass expansion factor (BEF) [35]. Belowground biomass (BGB), was estimated using a root-shoot ratio of 0.30 for sal and 0.26 for other species [36]. Total biomass of the sample plot was worked out by adding AGB, BGB, shrubs, herbs and litter biomass. Carbon was estimated as 47% of the total biomass [37].

The plot biomass values, thus obtained were brought to the geospatial domain for further use. All the geostatistical interpolation were performed using ArcGIS (ver. 10.2.2). For OK and UK, semi-variance analysis for characterizing the spatial auto-correlation of geolocated measurements, exponential, gaussian, circular, and spherical models were tested with the same number of lags and the same lag distances. All the above mentioned 16 variables were tested, one by one, as auxiliary variables in CoK. For fitting regionalization model, all direct semi-variograms and cross-semivariograms were estimated for the same number of lags and the lag distances. Then, the number and types of elementary models and their ranges were fixed. The sills (co-regionalization matrix) were fitted by trial and error. Among the 16 available auxiliary variables, three variables were selected for ReK based on the least Root Mean Square Error (RMSE) achiebved during CoK. The direct linear relationship between the field measured biomass and the variables were developed, and its corresponding residuals were obtained. The obtained linear equations were used for estimating the biomass for the entire study area. For ReK, the residuals found during linear fit was krigged using OK, then the obtained residual maps were added to the biomass map obtained from direct linear relationship. Thus, ReK biomass was obtained. The biomass maps produced by the described methods were evaluated and compared based on RMSE [38]. Finally, the spatial distribution of biomass with least RMSE was selected for estimation of spatial carbon stock of the study area.

3. Results and Discussion

3.1 Biomass mapping using univariate kriging techniques

To predict the value of the unknown position based on available information of known neighboring positions, spatial interpolation techniques are used. In the present study, the potential of simple univariate kriging methods (OK and UK) were tested with varying semivariogram models *viz*., spherical, exponential, Gaussian, and circular model. Exponential model was found as the best fit model based on Root Mean Square Standardized (RMSS) value (Table 2) for semi-variogram fitting and finally generated spatial biomass, however, both the univariate kriging methods failed in giving meaningful biomass estimate when evaluated with standard false colour composite of Landsat 8 (Fig. 1) and prior knowledge of study site.

Table 2: Different kriging model tested.

	Nugget	Partial sill	RMSS
Ordinary Kriging			
Spherical	0.365	0.350	1.02
Exponential	0.319	0.430	0.99
Gaussian	0.252	0.472	1.11
Circular	0.255	0.463	1.10
Universal Kriging			
Spherical	0.229	0.120	1.32
Exponential	0.255	0.092	1.31
Gaussian	0.259	0.091	1.33
Circular	0.252	0.097	1.33

RMSS = Root mean square standardized

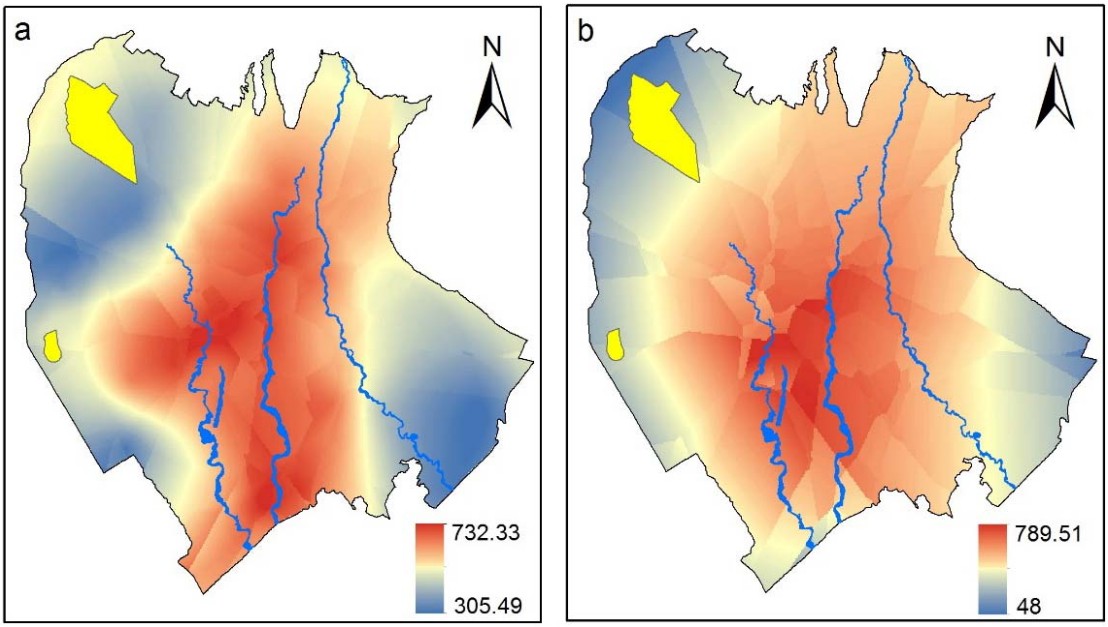

Fig 3: Biomass map (Mg ha^{-1}) generated using (a) OK (b) UK

It underestimated the biomass for the south-east and north-west direction of the study area. Fig. 3 (a) and (b) shows the spatial distribution of biomass through OK and UK. The overall RMSE observed against field validation points were 121.78 Mg ha^{-1} and 139.48 Mg ha^{-1} for OK and UK, respectively. The need of large dataset to define the spatial auto-correlation must have resulted to poor performance by OK and UK because the kriging coefficients entirely depend on the spatial variation. Because the variograms in OK and UK are fitted by the iterative weighted least square method, where the weights are calculated based on the number of sample points and the distances between the sample point pairs. Therefore, the accuracy of these methods depends on the number of sample points. So, evenly distributed sample points means more accurate information on spatial variability.

3.2 Evaluation of remotely sensed data as predictor variables of biomass

Large area forest inventory using remotely sensed data involves many challenges [39]. The heterogeneity of forest types some time makes difficult to relate with spectral responses of the remotely sensed data, especially when interpolation techniques are considered. One inherent source of bias when remote sensing data are linked with ground inventory data is the inconsistency between remotely sensed data and ground sampled data [39, 40]. Ground inventory data, collected at the forest plot level when linked with the representative pixel on the ground has some degree of error depending on the site homogeneity. Spatial diversity of forest stands and landscape are major challenges in spatial prediction of forest biophysical parameters. For example, forest stands may have very similar characteristics such as same species, same age, and same density but may have different spectral characteristics due to water Logging or very similar biomass but have different spectral signature because of differences in species composition. These differences increase uncertainty when ground-inventory data are associated with remotely sensed data for the prediction for forest parameters. To check the prediction capability of each variable, Pearson correlation coefficient (r) were calculated and their relation with biomass were judged based on the r value (Table 3). Among 16 test variables, the SWIR-2 band had the highest correlation (r = -0.45) with the total plot biomass and least correlation was observed with red band (r = 0.06).

Highest correlation of SWIR-2 with biomass must be due sensitivity of SWIR-2 with leaf moisture. In general theory, more number of leafs means more biomass, with increase in leafs more absorption of light in SWIR region, thereby decreasing reflectance in SWIR band. Hence, SWIR reflectance had negative correlation with biomass. Many studies have applied geostatistical techniques using the indices derived from the visible and near-infrared region (VNIR, 0.400–1.200 µm) *e.g.* [16-18-41]. However, in this study, it was observed that the use of SWIR (1.200–2.500 µm) or VIs obtained using SWIR region (*i.e.* LSWIs, MSI, and MIDIR) had lower RMSE than VNIR region or the VIs with VNIR region. The possible explanation for better performance of SWIR region could be attributed to,

1. more than 90% transmittance in SWIR region than VNIR,
2. the soil and vegetation reflectance at the SWIR are fairly strong and
3. SWIR region is less affected by aerosols [42, 43], and
4. Particularly during this study the sensitivity of SWIR to water might be the added advantage. Less ‘r’ value between biomass and other variables like Red, Green, NDVI, EVI, and WDRVI which are specific to leaf greenness must be due to the use of April data set as this period experiences yellowing and/or leaf fall. Yadav and Nandy [16] also found stronger relationship between plot biomass and SWIR than with Red, Green and NIR.

Table 3. Correlation between total biomass and remote sensing derived variables.

Variable	R	Variable	R
SWIR-2	-0.45	OSAVI	0.25
LSWI-2	0.44	RDVI	0.24
MIDIR	0.43	NDVI	0.19
MSI	-0.43	EVI	0.16
LSWI-1	0.39	WDRVI	0.16
SWIR-1	-0.38	GREEN	0.13
PC	-0.35	VARI	-0.09
NIR	0.34	RED	0.06

3.3 Biomass estimation using multivariate kriging

Traditional kriging uses only data available at the sampled location; CoK method instead uses the advantage of the covariance that exists between auxiliary variable and interest variable. CoK is a very versatile and rigorous statistical technique for spatial point estimation when both primary and auxiliary attributes are available [44]. The predictive capability of each auxiliary variable were tested in CoK. Among the 16 variables tested, lowest RMSE of 58.77 Mg ha^{-1} was found (Table 4).

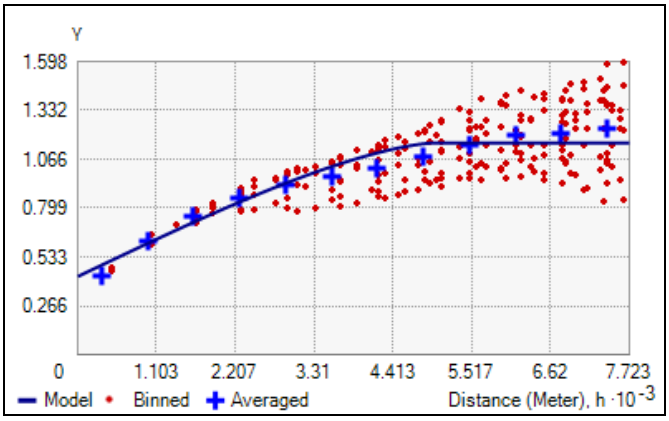

Fig 4: Best fit Semivariogram for LSWI-2.

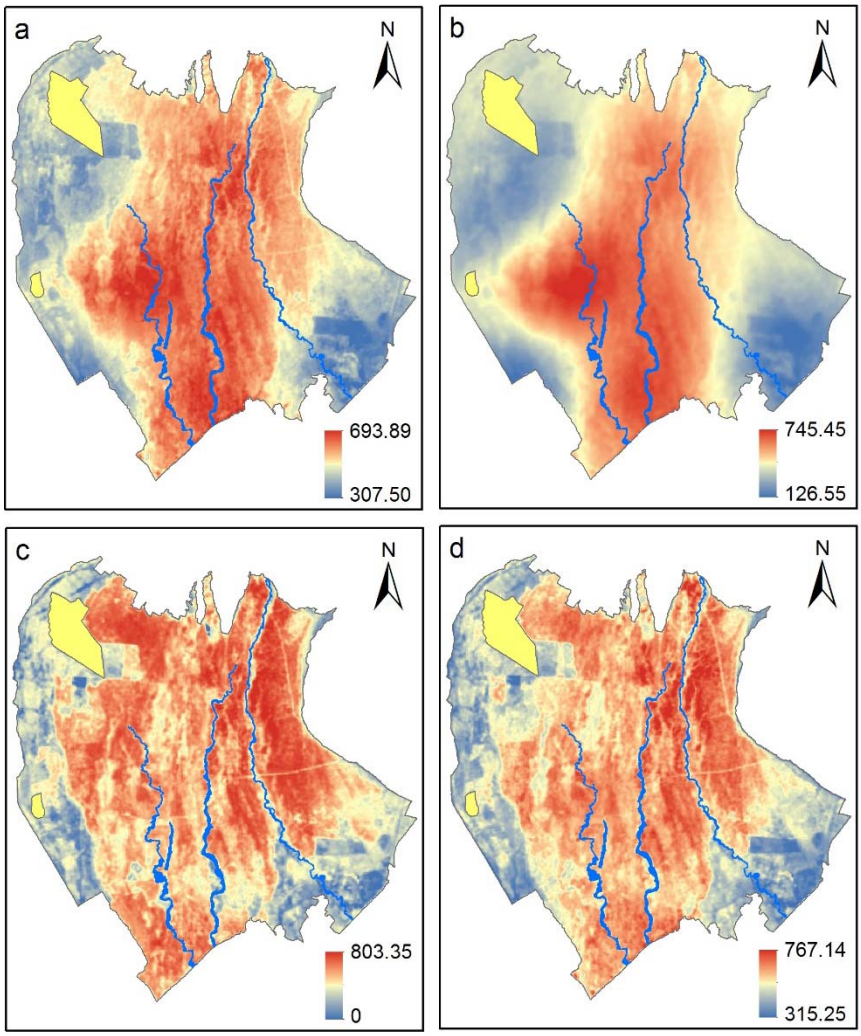

Fig 5: Cokrigged biomass (Mg ha^{-1}) map using (a) NIR (b) PC (c) LSWI-2 and (d) OSAVI

Table 4: RMSE (Mg ha^{-1}) and R^2 observed between CoK biomass and validation points.

Variable	RMSE	R^2	Variable	RMSE	R^2
LSWI-2	58.77	0.63	RDVI	82.13	0.18
SWIR-2	63.06	0.50	WDRVI	83.79	0.15
MIDIR	63.50	0.31	NDVI	84.14	0.14
LSWI-1	64.64	0.70	EVI	90.20	0.20
MSI	64.65	0.70	Red	100.59	-0.05
SWIR-1	71.72	0.53	NIR	105.81	0.05
PC	75.80	0.30	VARI	108.63	0.11
OSAVI	79.71	0.25	Green	109.24	-0.64

Fig. 4 shows the best fit covariance model of LSWI-2 with total sample plot biomass. Co-Krigged spatial biomass using different satellite derived auxiliary variables is given in Fig. 5.

For ReK, LSWI-2, SWIR-2, and MIDIR were selected as auxiliary variables by lowest RMSE observed during CoK (Table 4). At first, the linear fit equation observed between biomass and auxiliary variables were used for estimating the forest biomass. Linear fit estimated spatial biomass had RMSE of 114.74 Mg ha^{-1}, 122.30 Mg ha^{-1} and 108.05 Mg ha^{-1} for LSWI-2, SWIR-2, and MIDIR, respectively. To obtain ReK biomass, the residuals obtained during the linear fit were used as an input variable in OK to generate the error/residual map and then generated residual was added to linear fit obtained biomass, thus ReK spatial biomass was obtained.

Table 5: Linear fit equation used in ReK and its RMSE.

Independent variable	Linear fit function	RMSE (Mg ha^{-1})
LSWI-2	Biomass = 272.90 + 499.99 × LSWI-2	122.26
SWIR-2	Biomass = 782.59 - 3008.24 × SWIR-2	128.40
MIDIR	Biomass = -113.50 + 323.60 × MIDIR	128.46

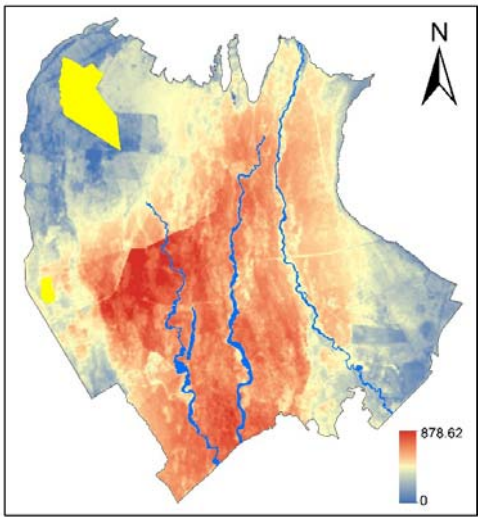

Fig 6: Regression krigged biomass (Mg ha^{-1}) map using LSWI-2.

It was observed that the RMSE obtained through ReK were higher than RMSE obtained using direct linear relationship and double the time of the RMSE obtained through CoK. The linear fit equation used in the ReK and the observed RMSE is given Table 5. The ReK estimated spatial biomass using LSWI-2 residual is shown in Fig. 6.

The possible cause for higher RMSE may be, in ReK its main coefficients, except the coefficient of the residual part, depend on the linear correlation between dependent and independent variables [19]. In case of the area with high spectral variability, the use of linear fit May over or underestimate the forest parameters, or the added OK residual value inherited typical kriging models limitation.

Through CoK, both the predicting capability of the auxiliary variables and the spatial-autocorrelation that exist in this study site was utilized. Therefore, CoK technique surpasses the ReK performance. According to Eldeiry *et al.* [45], CoK works best compared to other geostatistical tools when the primary variable of interest is not densely sampled.

The reason for best performance by LSWI-2 was the sensitivity of this index with water content, as discussed in section 3.2. LSWI can be considered to equivalent water thickness (g H_2O/m^2) [46]. Work done by Maki *et al.*, [47] and Xiao *et al.*, [48] in evergreen needle leaf forests have shown the sensitive of LSWI with changes in leaf water content. With increase and decrease in leaf liquid water content or soil moisture, SWIR absorption increases and decreases thereby decreasing and increasing reflectance in SWIR band, resulting in an increase and decrease in LSWI value. LSWI is useful in extracting the vegetation water status and in drought detection and water sustainability studies [49]. Xiao *et al.* [46-48] used LSWI as an index for defining water scalar in satellite-based Vegetation Photosynthesis Model (VPM) for estimation of gross primary productivity.

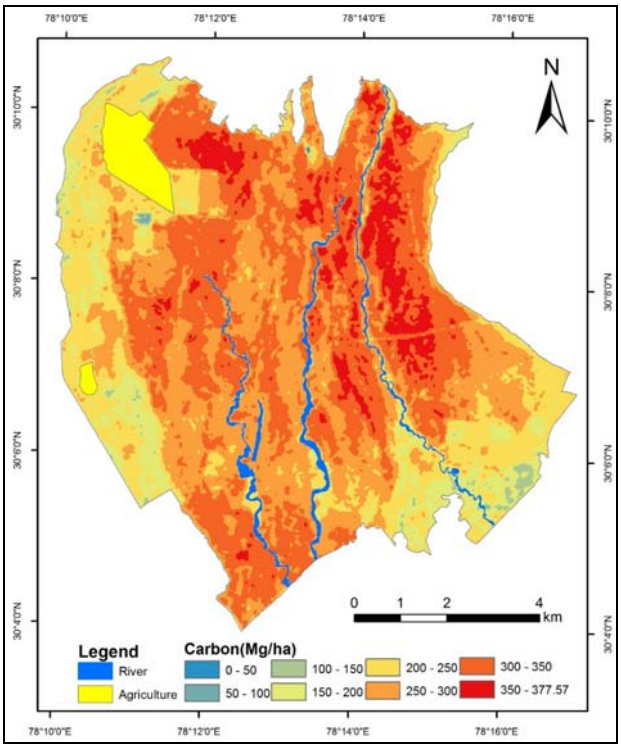

Fig 7: Total carbon stock map of Barkot forest.

The co-krigged biomass using LSWI-2 as an auxiliary variable gave the best estimate and subsequently was used for spatial mapping of forest carbon stock (Fig. 7). Maximum plot biomass observed in Barkot forest was 803.35 Mg ha^{-1}, Yadav and Nandy, [16] reported maximum plot biomass of 421 Mg ha^{-1} AGB for a sal forest, considering an average BEF of 1.5 and root-shoot ratio of 30%, maximum total plot biomass will be approx. 820.95 Mg ha^{-1} which agrees with our finding. The total carbon stored by Barkot forest (excluding agriculture and water body) was estimated to be 2240797.37 Mg C, with an average of 276.13 Mg C ha^{-1}. A very close estimate was reported by Mandal and Joshi [50] for a similar forest (located very close to the present study area) with a carbon density of 280.78 Mg C ha^{-1} using only field inventory methods.

4. Conclusion

The use of satellite derived information as secondary data for forest biomass estimation not only helps in generating a continuous spatial biomass map but also in obtaining more accuracy. Geostatistical prediction techniques provide a better way to estimate spatially forest biomass/carbon when ground inventory data and remotely sensed data are available. This approach can be applied in other research areas, for many applications in the forest or natural resource management such as forest health conditions, leaf area index, stand age, etc. while correlation analysis, best fit semivariogram/covariance models, and kriging models need to be examined for spatial estimation. Among the univariate kriging, OK had lesser RMSE than UK. ReK estimated biomass had higher RMSE value than biomass estimated using direct linear relationship equation observed between satellites derived variables and the plot biomass. CoK was noticed to the most powerful one among the different kriging methods adopted in this study. Out of 16 auxiliary variables tested in CoK, least RMSE of 58.77 Mg ha^{-1} was found with LSWI-2. We also found SWIR or SWIR based indices performed better in the prediction of total biomass. The total carbon stored by Barkot forest excluding agriculture and water body was estimated to be 2240797.37 Mg C, with an average of 276.13 Mg C ha^{-1} which accords with the other recent studies in moist sal forest. Reliable spatial information of biomass and carbon is essential for better forest carbon management and planning. This information on spatial biomass/carbon will be used in complementing carbon flux studies at BFS.

5. Acknowledgements

The present work was carried out as part of National carbon project under ISRO-Geosphere Biosphere Program (IGBP). The authors wish to acknowledge Dr. V. K. Dadhwal, Project director (NCP-IGBP), Dr. A. Senthil Kumar, Director IIRS, Divisional Forest Officer, Dehradun Forest Division and staff Barkot and Rishikesh Range, Dehradun Forest Division of the Government of Uttarakhand, India for field support.

6. Reference

1. Sales MH, Souza Jr CM, Kyriakidis PC, Roberts DA, Vidal E. Improving spatial distribution estimation of forest biomass with geostatistics: a case study for rondônia, Brazil. Ecological Modeling 2007; 205:221-230.
2. Franco-Lopez H, Ek AR, Bauer ME. Estimating and mapping of forest stand density, volume, and cover type using the k-nearest neighbours method. Remote Sensing of Environment. 2001; 77:251-274.
3. Caputo J. Sustainable forest biomass: promoting renewable energy and forest stewardship. Policy paper, Environmental and Energy Study Institute, 2009.
4. UNFCCC. Methodological Guidance for Activities Relating to Reducing Emissions from Deforestation and Forest Degradation and The role of Conservation, Sustainable Management of Forests and Enhancement of Forest Carbon Stocks in Developing Countries; Draft Decision/CP.15; Advanced unedited version, UNFCCC: Bonn, Germany, 2009.
5. McRoberts RE, Cohen WB, Naesset E, Stehman SV, Tomppo EO. Using remotely sensed data to construct and assess forest attribute maps and related spatial products. Scandinavian Journal of Forest Research. 2010; 25:340-367.
6. Maynard CL, Lawrence RL, Nielsen GA, Decker G. Modeling vegetation amount using band-wise regression and ecological site descriptions as an alternative to vegetation indices. GIScience & Remote Sensing. 2007; 44:68-81.
7. Main-Knorn M, Moisen GG, Healey SP, Keeton WS, Freeman EA, Hostert P. Evaluating the remote sensing and inventory-based estimation of biomass in the Western Carpathians; Remote Sensing 2011; 3:1427-1446.
8. Kushwaha SPS, Nandy S, Gupta M. Growing stock and woody biomass assessment in Asola-Bhatti Wildlife Sanctuary, Delhi, India; Environmental Monitoring and Assessment 2014; 186(9):5911-5920.
9. Mitchard ETA, Saatchi S, White LJT, Abernethy KA, Jeffery KJ, Lewis SL, *et al*. mapping tropical forest biomass with radar and space borne LiDAR in Lopè National Park, Gabon: overcoming problems of high biomass and persistent cloud; Biogeosciences. 2012; 9:179-191.
10. Eckert S. Improved Forest Biomass and Carbon Estimations Using Texture Measures from WorldView-2 Satellite Data. Remote Sensing. 2012; 4:810-829.
11. Manna S, Nandy S, Chanda A, Akhand A, Hazra S, Dadhwal VK. Estimating aboveground biomass in Avicennia marina plantation in Indian Sundarbans using high-resolution satellite data. Journal of Applied Remote Sensing. 2014; 8:1-12.
12. Heyjoo BP, Nandy S. Estimation of above-ground phytomass and carbon in tree resources outside the forest (TROF): A geo-spatial approach. Banko Janakari. 2014; 24(1):34-40.
13. Lu D. Aboveground biomass estimation using Landsat TM data in the Brazilian Amazon. International Journal of Remote Sensing. 2005; 26:2509-2525.
14. Nelson RF, Kimes DS, Salas WA, Routhier M. Secondary forest age and tropical forest biomass estimation using Thematic Mapper imagery. Biogeosciences. 2000; 50:419-431.
15. Corona P, Chirici G, McRoberts RE, Winter S, Barbati A. Contribution of large-scale forest inventories to biodiversity assessment and monitoring; Forest Ecology and Management. 2011; 262:2061-2069.
16. Yadav BKV, Nandy S. Mapping aboveground woody biomass using forest inventory, remote sensing and geostatistical techniques. Environmental Monitoring and Assessment. 2015; 187:308. DOI 10.1007/s10661-015-4551-1
17. Blodgett C, Jakubauskas M, Price K, Martinko E. Remote Sensing-based Geostatistical Modeling of Forest Canopy Structure; ASPRS Annual Conference Washington, DC, 2000.
18. Corona P, Fattorini L, Franceschi S, Chirici G, Maselli F, Secondi L. Mapping by spatial predictors exploiting remotely sensed and ground data: A comparative design-based perspective. Remote Sensing of Environment. 2014; 152:29-37.
19. Meng Q, Cieszewski C, Madden M. Large area forest inventory using Landsat ETM+: A geostatistical approach. ISPRS Journal of Photogrammetry and Remote Sensing. 2009; 64: 27-36.

20. Ver-Hoef JM, Temesgen H. A comparison of the spatial linear model to nearest neighbor (k-NN) methods for forestry applications; PLoS ONE. 2013; 8:e59129.
21. Tsui OW, Coops NC, Wulder MA, Marshall PL. Integrating airborne LiDAR and space-borne radar via multivariate kriging to estimate above-ground biomass; Remote Sens. Environ. 2013; 139:340-352.
22. Champion HG, Seth SK. A revised survey of the forest types of India. New Delhi: Manager of Publications, Government of India, 1968.
23. Chacko VJ. A manual on sampling techniques for forest surveys. New Delhi: Manager of Publications, Government of India, 1965.
24. Musick HB, Pelletier RE. Response to soil moisture of spectral indexes derived from bidirectional reflectance in Thematic Mapper wavebands. Remote Sensing of Environment. 1988; 25:167-184.
25. Hunt Jr E, Rock B. Detection of Changes in Leaf Water Content Using Near- And Middle-Infrared Reflectances. Remote Sensing of Environment. 1989; 30:43-54.
26. Xiao X, Boles S, Frolking S, Salas W, Moore B, Li C, *et al*. Landscape-scale characterization of cropland in China using Vegetation and Landsat TM images; International Journal of Remote Sensing. 2002; 23:3579-3594.
27. Rouse JW, Haas RH, Schell JA, Deering DW, Harlan JC. Monitoring the vernal advancements and retrogradation of natural vegetation; In: NASA/GSFC, Final Report, Greenbelt, MD, USA, 1974.
28. Peng Y, Gitelson AA. Application of chlorophyll-related vegetation indices for remote estimation of maize productivity; Agriculture and Forest Meteorology. 2011; 151:1267-1276.
29. Huete A, Didan K, Miura T, Rodriguez EP, Gao X, Ferreira LG. Overview of the radiometric and biophysical performance of the MODIS vegetation indices. Remote Senssing of Environment 2002; 83:195-213.
30. Gitelson A, Stark R, Grits U, Rundquist D, Kaufman Y, Derry D. Vegetation and Soil Lines in Visible Spectral Space: A Concept and Technique for Remote Estimation of Vegetation Fraction; International Journal of Remote Senssing. 2002; 23(13):2537-2562.
31. Rougean JL, Breon FM. Estimating PAR absorbed by vegetation from bidirectional reflectance measurements. Remote Sensing of Environment. 1995; 51:375-384.
32. Rondeaux G, Steven M, Baret F. Optimization of soil-adjusted vegetation indices; Remote Sensing of Environment. 1996; 55:95-107.
33. FSI. Volume equations for forests of India, Nepal and Bhutan. Dehradun: Forest Survey of India, Ministry of Environment and Forests, Government of India, 1996.
34. FRI. Indian woods: their identification, properties and uses, (Revised edition). Dehradun: Forest Research Institute, Indian Council of Forestry Research and Education, Ministry of Environment and Forests, Government of India, 2002, I-VI
35. Haripriya GS. Estimates of biomass in Indian forests. Biomass and Bioenergy. 2000; 19(4):245-258.
36. Negi JDS. Biological productivity and cycling of nutrients in managed and man-made ecosystems; Ph.D. Thesis, Garhwal University, Srinagar, India, 1984.
37. IPCC. IPCC guidelines for national greenhouse gas inventories, Prepared by the National Greenhouse Gas Inventories Programme, Eggleston HS, Buendia L, Miwa K, Ngara T, Tanabe K (eds) Published: IGES, Japan, 2006.
38. Fazakas Z, Nilsson M, Olsson H. Regional forest biomass and wood volume estimation using satellite data and ancillary data; Agriculture and Forest Meteorology. 1999; 98-99:417-425.
39. Tokola T, Pitkänen S, Partinen S, Muinonen E. Point accuracy of a nonparametric method in estimation of forest characteristics with different satellite materials; International Journal of Remote Sensing. 1996; 17(12):2333-2351.
40. Gilbert B, Lowell K. Forest attributes and spatial autocorrelation and interpolation: Effects of alternative sampling schemata in the boreal forest. Landscape Urban Plan. 1997; 37:235-244.
41. Singh TP, Das S. Predictive Analysis for Vegetation Biomass Assessment in Western Ghat Region (WG) Using Geospatial Techniques. Journal of the Indian Society of Remote Sensing. 2013; 423:549-557.
42. Karnieli A, Kaufman Y, Remer L, Wald A. AFRI – Aerosol Free Vegetation Index. Remote Senssing and Environment. 2001; 77:10-21.
43. Ben-Ze'ev E, Karnieli A, Agam N, Kaufman Y, Holben B. Assessing vegetation condition in the presences of biomass burning smoke by applying the Aerosol-free Vegetation Index (AFRI) on MODIS images; International Journal of Remote Sensing. 2006; 27:3203-3221.
44. Vauclin M, Vieira SR, Vachaud G, Nielsen DR. The use of cokriging with limited field soil observations. Soil Science Society of America Journal. 1983; 47(2)175-184.
45. Eldeiry A, Garcia LA. Comparison of regression kriging and cokriging techniques to estimate soil salinity using Landsat images; Civil and Environmental Engineering Department, Colorado State University, Fort Collins, CO 80523–1372, Hydrology Day, 2009.
46. Xiao XM, Zhang QY, Saleska S, Hutyra L, Camargo P, Wofsy S, *et al*. Satellite-based modeling of gross primary production in a seasonally moist tropical evergreen forest; Remote Sensing of Environment. 2005; 94:105-122.
47. Maki M, Ishiahra M, Tamura M. Estimation of leaf water status to monitor the risk of forest fires by using remotely sensed data; Remote Sensing of Environment. 2004; 90:441-450.
48. Xiao XM, Zhang QY, Hollinger D, Aber J, Moore B. Modeling gross primary production of an evergreen needleleaf forest using MODIS and climate data. Ecological Applications. 2004; 15(3):954-969.
49. Kim H, Huete R, Nagler PN, Glenn E, Emmerich W. Scott RL. Monitoring riparian and semi-arid upland vegetation using vegetation and water indices from the MODIS satellite sensor. In Research Insights in Semiarid Ecosystems (RISE) University of Arizona, Tucson, 2004.
50. Mandal G, Joshi SP. Estimation of above-ground biomass and carbon stock of an invasive woody shrub in the subtropical deciduous forests of Doon Valley, western Himalaya, India. International Journal of Environmental Biology. 2014; 4(2):157-169.